MMSE Precoding for Receive Spatial Modulation in Large MIMO Systems

Ahmed Raafat, Adrian Agustin and Josep Vidal
Dept. of Signal Theory and Communications, Universitat Politecnica de Catalunya (UPC), Barcelona, Spain.
Email: {ahmed.raafat, adrian.agustin, josep.vidal}@upc.edu

***Abstract*—Receive spatial modulation (RSM) schemes enable simple and energy efficient multiple-input-multiple-output (MIMO) transceivers and yet attain high spectral efficiency, which renders them promising schemes for millimeter wave (mmWave) communication in massive MIMO systems. When these schemes are designed to include zero forcing (ZF) precoders, performance can be impaired in the presence of highly spatially correlated channels. Extending these schemes for minimum mean square error (MMSE) precoding is not trivial due to the hardware constraints of the energy efficient user terminal architecture. In this paper, we adapt the MMSE precoder to the low complexity RSM architecture and develop detection methods for the spatial and modulation symbols. The proposed MMSE RSM scheme with total and per-antenna power constraints have been compared with ZF RSM in terms of average and outage mutual information by simulations showing superior gain for mmWave channels.**

***Index Terms*—RSM, MMSE, Massive MIMO, mmWave.**

I. Introduction

Receive spatial modulation (RSM) schemes can leverage receive antenna array as an extra information source to attain high spectral efficiency [1] and superior energy efficiency compared with hybrid MIMO. In RSM, the base station (BS) maps the input data into two streams, spatial stream that conveys the indices of the active receive antennas and modulation stream for e.g., M-ary symbols. These schemes have been introduced for sub-6 GHz communication considering fully digital (FD) multiple-input-multiple-output (MIMO) transceiver architecture [2]-[3]. Recently, RSM schemes have been proposed for indoor line-of-sight [4] and outdoor narrowband [5] in millimeter wave (mmWave) propagation environment by applying zero forcing (ZF) precoding. However, ZF precoding is challenging if the channel is spatially correlated: badly conditioned solutions and low signal-to-noise-ratio (SNR) at the receiver are obtained. Thus, efficient receive antenna selection (RAS) algorithms based ZF precoding have been developed in [6] to enhance the RSM performance in the spatially correlated channels.

Adapting the RSM scheme in [5] to minimum mean square error (MMSE) precoding is not straightforward due to the user terminal (UT) hardware constraints (one radio-frequency (RF) chain) in Fig. 1 and the unavailability of channel state information (CSI) at the UT. In ZF RSM, no CSI is needed at the UT for phase compensation to the modulation symbol [5]. In contrast, the UT for MMSE RSM needs partial channel knowledge for modulation symbol phase compensation that could increase the training overhead. In this paper, we provide detection solutions at the UT to efficiently adapt the MMSE precoding with the energy efficient RSM architecture in Fig. 1. The novelty and contribution of this paper are as follows

- We derive semi-closed form expression for the maximum likelihood (ML) spatial symbol detector that can be evaluated numerically and high SNR closed form expression.
- We develop modulation symbol detection scheme such that blind phase compensation is performed at the UT.
- We perform RAS method to maximize the mutual information based on exhaustive search and show that the RAS is needed for MMSE RSM system operating in spatially correlated channels.
- We show that the proposed MMSE RSM scheme with total power constraint (TPC) and with per antenna power constraint (PAPC) at the BS outperforms the ZF RSM in terms of average and outage mutual information.

II. System model

We consider the downlink (DL) of a massive MIMO single user system operating in outdoor environment, narrowband transmission at mmWave frequencies. The UT and the BS are equipped with N_r and N_t antennas, respectively. The proposed modulation scheme could be extended to wideband propagation by applying time domain precoding for single carrier systems. We consider FD BS and energy efficient UT circuit as depicted in Fig. 1.

A. Channel model

Outdoor propagation of mmWave signals suffers from severe path loss and tiny reflection coefficients in obstacles, thus the channel is limited by few scattering clusters. Therefore, we adopt the outdoor and narrowband channel model [7] in evaluating the proposed algorithms performance. According to this model, the channel matrix can be expressed as

$$\mathbf{H} = \sqrt{\frac{N_t N_r}{L}} \sum_{i=1}^{L} g_i \mathbf{v}_r\left(\theta_i\right) \mathbf{v}_t\left(\phi_i\right)^H \tag{1}$$

where $\mathbf{H} \in \mathbb{C}^{N_r \times N_t}$, L is number of effective scattering paths, (g_i, ϕ_i, θ_i) are the i^{th} path gain, azimuth angle of departure, elevation angle of arrival, respectively, $\left(\mathbf{v}_t\left(\phi_i\right), \mathbf{v}_r\left(\theta_i\right)\right)$ are

The research leading to these results has been partially funded by the 5Gwireless project within the framework of H2020 Marie Skłodowska-Curie innovative training networks (ITNs), the project 5G&B RUNNER-UPC (TEC2016-77148-C2-1-R (AEI/FEDER, UE)) and the Catalan Government (2017 SGR 578-AGAUR).

the the i^{th} path transmit and receive uniform linear array (ULA) response vectors. The N-antennas ULA response vector can be expressed as

$$\mathbf{v}(\phi) = \frac{1}{\sqrt{N}}\left[1, e^{jkd\sin(\phi)}, ..., e^{j(N-1)kd\sin(\phi)}\right]^T \quad (2)$$

where $k = \frac{2\pi}{\lambda}$ and d is the inter-antennas spacing.

B. Bit to symbol mapping

In [5], the BS transmits two symbols per channel use, spatial symbol $\mathbf{s}_i \in \mathbb{R}^{N_r \times 1}$ comprises N_r input bits and modulation symbol x_j from M-ary constellation. The transmit vector at the precoder input is $(\mathbf{x}_i^j = \mathbf{s}_i x_j)$ where the number of transmit bits per channel use equal $(N_r + \log_2 M)$. According to this mapping, we lose x_j if $\mathbf{s}_i$ is all zeros vector. Hence, in [5], the authors assume that the all zeros $\mathbf{s}_i$ is not allowed. However, this assumption entails significant spectral efficiency loss if N_r is small. Thus, we modify this mapping such that

$$\mathbf{x}_i^j = \begin{cases} \mathbf{s}_i x_j & \text{if} \quad \mathbf{s}_i \neq \mathbf{0}_{N_r} \\ \mathbf{s}_i & \text{if} \quad \mathbf{s}_i = \mathbf{0}_{N_r} \end{cases} \quad (3)$$

we consider the all zeros $\mathbf{s}_i$ but do not transmit x_j with it.

C. System assumptions

Channel reciprocity at mmWave propagation motivates using time-division-duplex protocol where the CSI is needed at the BS side only. The BS can acquire the CSI during the uplink (UL) training interval with low overhead [5]. Small number of DL training symbols are needed for design the UT detection as illustrated in section (IV-C). Transmissions assume a block fading channel model, where the channel remains constant during the channel coherence time and is independent from block to block. In each block, the channel estimation, UL and DL transmissions are carried out.

III. Precoding

The received signal vector can be expressed as

$$\mathbf{y} = \mathbf{H}\mathbf{P}\mathbf{s}_i x_j + \mathbf{n} \quad (4)$$

where $\mathbf{n} \in \mathbb{C}^{N_a \times 1}$ is a noise vector has independent and identically distributed $\mathcal{CN}\left(0, \sigma^2\right)$ entries, the precoding matrix $\mathbf{P} \in \mathbb{C}^{N_t \times N_a}$ is fixed during the coherence time and satisfies

$$\mathrm{E}\left[\|\mathbf{P}\mathbf{s}_i x_j\|_2^2\right] = \mathrm{Tr}\left\{\mathbf{P}\mathbf{R}_{ss}\mathbf{P}^H\right\} = P_t. \quad (5)$$

where $\mathbf{R}_{ss} = \mathrm{E}\left[\mathbf{s}_i \mathbf{s}_i^H\right]$ and P_t is the transmit power.

In the sequel, we consider MMSE precoding with PAPC and TPC and develop the detection technique. Let us consider the MMSE precoding matrix $(\mathbf{P} = \tilde{\mathbf{P}}/\sqrt{\beta})$ where β is used for adjusting the transmit power at the BS and for scaling the desired signal at the UT [8]. The MSE can be expressed as

$$\mathrm{E}\left[\left\|\sqrt{\beta}\mathbf{y} - \mathbf{s}_i x_j\right\|_2^2\right] = \left\|(\mathbf{H}\tilde{\mathbf{P}} - \mathbf{I}_{N_r})\mathbf{R}_{ss}^{\frac{1}{2}}\right\|_F^2 + \sigma^2 N_r \beta \quad (6)$$

As it will be illustrated in section (IV-B), the matrix $\mathbf{HP}$ has to be symmetric to allow blind phase compensation to the

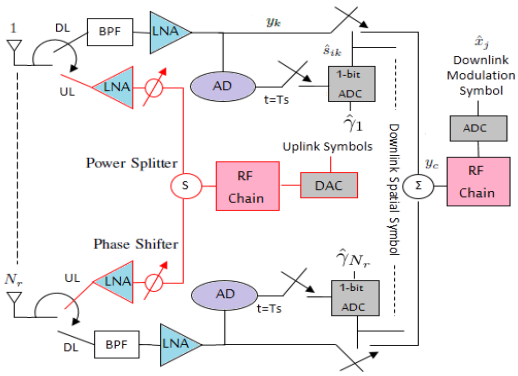

Fig. 1. RSM transceiver architecture introduced in [5].

modulation symbol. Thus, the design problem of the MMSE precoder with PAPC (MMSEPAPC) can be expressed as

$$\text{(P1)} \begin{cases} \min\limits_{\tilde{\mathbf{P}},\beta} & \left\|(\mathbf{H}\tilde{\mathbf{P}} - \mathbf{I}_{N_r})\mathbf{R}_{ss}^{\frac{1}{2}}\right\|_F^2 + \sigma^2 N_r \beta \\ \text{s.t.} & \left[\tilde{\mathbf{P}}\mathbf{R}_{ss}^{\frac{1}{2}}\right]_{(k,:)}^H \left[\tilde{\mathbf{P}}\mathbf{R}_{ss}^{\frac{1}{2}}\right]_{(k,:)} \leqslant \beta\frac{P_t}{N_t}, \\ & \qquad\qquad k = 1, \cdots, N_t. \\ & \mathbf{H}\tilde{\mathbf{P}} = \tilde{\mathbf{P}}^H\mathbf{H}^H. \end{cases} \quad (7)$$

where problem (P1) is convex quadratic constrained quadratic program that can be solved by software packages like CVX [9]. A closed form expression of the MMSE precoder with TPC (MMSETPC) [8] can be obtained by replacing the PAPC in problem (P1) with a TPC $(\mathrm{Tr}\{\tilde{\mathbf{P}}\mathbf{R}_{ss}\tilde{\mathbf{P}}^H\} \leqslant \beta P_t)$ and dropping the symmetry constraint $(\mathbf{H}\tilde{\mathbf{P}} = \tilde{\mathbf{P}}^H\mathbf{H}^H)$ as follows

$$\begin{aligned} \tilde{\mathbf{P}} &= \mathbf{H}^H\left(\mathbf{H}\mathbf{H}^H + \frac{\sigma^2 N_r}{P_t}\mathbf{I}_{N_r}\right)^{-1} \\ \beta &= \mathrm{Tr}\{\tilde{\mathbf{P}}\mathbf{R}_{ss}\tilde{\mathbf{P}}^H\}/P_t \end{aligned} \quad (8)$$

Although we drop the symmetry constraint, the precoder in equation (8) satisfies the symmetric property $(\mathbf{H}\tilde{\mathbf{P}} = \tilde{\mathbf{P}}^H\mathbf{H}^H)$ as illustrated in the sequel.

$$\begin{aligned} \mathbf{H}\tilde{\mathbf{P}} &= \mathbf{H}\mathbf{H}^H\left(\mathbf{H}\mathbf{H}^H + c\mathbf{I}_{N_r}\right)^{-1} \\ \tilde{\mathbf{P}}^H\mathbf{H}^H &= \left(\mathbf{H}\mathbf{H}^H + c\mathbf{I}_{N_r}\right)^{-1}\mathbf{H}\mathbf{H}^H \end{aligned} \quad (9)$$

According to the matrix inversion lemma [10]

$$\mathbf{A}\left(\mathbf{A} + c\mathbf{I}_{Nr}\right)^{-1} = \left(\mathbf{A} + c\mathbf{I}_{Nr}\right)^{-1}\mathbf{A} \quad (10)$$

equation (9) shows that $\mathbf{H}\tilde{\mathbf{P}}$ is symmetric.

IV. Detection

The received signal by the k^{th} antenna can be expressed as

$$y_k = \underbrace{[\mathbf{HP}]_{k,k}\, s_{ik} x_j + \sum_{l \neq k} [\mathbf{HP}]_{k,l}\, s_{il} x_j}_{r_k} + n_k \quad (11)$$

where s_{ik} is the k^{th} bit of the spatial symbol $\mathbf{s}_i$.

The spatial symbol detection based on joint processing of the signals received by all antennas requires complex receiver

architecture. For the sake of reducing the receiver hardware complexity, we consider per antenna spatial symbol detection where we can exploit energy efficient devices (amplitude detectors (ADs), 1-bit ADCs) represented in Fig. 1 in the spatial symbol detection. The output signal from the k^{th} AD can be expressed as

$$a_k = |y_k| \tag{12}$$

The probability density function of the k^{th} received amplitude (a_k) given the k^{th} transmit spatial bit (s_{ik}) is

$$f(a_k \mid s_{ik} = m) = \sum_{i=1}^{2^{N_r-1}} f(a_k \mid s_{ik}, \tilde{\mathbf{s}}_i)\Pr(\tilde{\mathbf{s}}_i) \tag{13}$$

where $\tilde{\mathbf{s}}_i \in \mathbb{R}^{N_r-1\times 1}$ equals $\mathbf{s}_i$ without s_{ik} and $m \in \{0,1\}$. Equation (13) is weighted sum of Rice distributions [11] and can be expressed as

$$f(a_k|s_{ik}{=}m){=}\frac{1}{2^{N_r-1}}\sum_{i=1}^{2^{N_r-1}}\frac{2a_k}{\sigma^2}e^{-\frac{a_k^2+a_{m,ik}^2}{\sigma^2}}\mathrm{I}_0\left(\frac{2a_k a_{m,ik}}{\sigma^2}\right) \tag{14}$$

where $a_{m,ik} = \left|r_{k|s_{ik}=m}\right|$ and $\mathrm{I}_0(x)$ is the zero order modified bessel function of the first kind.

A. Spatial symbol detection

The received spatial bit per antenna can be either one or zero, thus we can detect it by applying ML detector per receive antenna as follows

$$f(a_k|s_{ik}=1)\underset{\hat{s}_{ik}=0}{\overset{\hat{s}_{ik}=1}{\gtrless}} f(a_k|s_{ik}=0) \tag{15}$$

$$\hat{s}_{ik} = \begin{cases} 1 & \text{if } a_k > \gamma_k \\ 0 & \text{if } a_k < \gamma_k \end{cases}, \gamma_k = \left\{ a_k \left| \frac{f(a_k|s_{ik}=1)}{f(a_k|s_{ik}=0)} = 1 \right. \right\} \tag{16}$$

$$\gamma_k = \left\{ a_k \left| \frac{\sum_{i=1}^{2^{N_r-1}} e^{-\frac{a_{1,ik}^2}{\sigma^2}}\mathrm{I}_0\left(\frac{2a_k a_{1,ik}}{\sigma^2}\right)}{\sum_{i=1}^{2^{N_r-1}} e^{-\frac{a_{0,ik}^2}{\sigma^2}}\mathrm{I}_0\left(\frac{2a_k a_{0,ik}}{\sigma^2}\right)} = 1 \right. \right\} \tag{17}$$

where equation (17) can be solved numerically at the BS to obtain γ_k, then the BS informs the UT about γ_k through low DL training overhead.

Approximate γ_k: with the aim of reducing the computational complexity at the BS, γ_k can be obtained in closed form by applying the high SNR assumption (HSA) $(\mathrm{I}_0(x) \approx \frac{e^x}{\sqrt{2\pi x}})$ to $f(a_k|s_{ik}=1)$ as follows

$$f(a_k|s_{ik}=1) \propto e^{-\frac{\min\left(a_{1,ik}^2\right)-2\min\left(a_{1,ik}\right)\gamma_k}{\sigma^2}} \tag{18}$$

where at high SNR the exponential term in equation (18) tends to zero or infinity if the exponent is negative or positive, respectively. Thus, the HSA threshold can be expressed as

$$\gamma_k \approx \frac{1}{2}\min(a_{1,ik}) \tag{19}$$

B. Modulation symbol detection

We consider one RF chain and one high precision analog-to-digital-converter (ADC) at the UT to detect the modulation symbol x_j. In order not to accumulate noise at the RF chain, $\hat{s}_{ik}$ controls switch in such a way that y_k goes to the RF chain only if $\hat{s}_{ik} = 1$. The combined signal y_c (shown in Fig. 1) can be expressed as

$$y_c = \sum_{k=1}^{N_r} \hat{s}_{ik} y_k = \alpha_i x_j + n_c \tag{20}$$

where α_i is a complex gain and n_c is the combined noise.

Worst case detection: In the worst case, we can detect the modulation symbol x_j only if the detected spatial symbol is error free $(\hat{s}_{ik} = s_{ik})$. In this case, we show that the phase of the modulation symbol does not change after combining and as a result no phase compensation is needed. From equations (11) and (20), α_i without spatial errors, can be expressed as

$$\alpha_i = \sum_{k\in\{s_{ik}=1\}} [\mathbf{HP}]_{k,k} + \frac{1}{2}\sum_{\substack{k\in\{s_{ik}=1\} \\ l\in\{s_{ik}=1\}, l\neq k}} [\mathbf{HP}]_{k,l} + [\mathbf{HP}]_{l,k} \tag{21}$$

Thanks to the symmetry of the matrix $\mathbf{HP}$, α_i in equation (21) becomes real positive gain, and therefore the phase of x_j in equation (20) does not change after combining.

C. Estimation of the detection thresholds

The UT needs the thresholds $(\gamma_1, \cdots, \gamma_{N_r})$ obtained in equation (17) for spatial symbol detection. During the DL training, the BS sends these thresholds to the UT. The accuracy of the estimated thresholds affect the system performance, thus the DL pilot symbols are designed in such a way that the k^{th} received signal vector can be expressed as

$$\mathbf{y}_{k,dl} = \gamma_k \mathbf{1}_{N_r} + \mathbf{n} \tag{22}$$

A closed form for the ML estimator $(\hat{\gamma}_k)$ has been proved in equation (33) in [5]. The number of needed pilot symbols is N_r to estimate N_r distinct thresholds.

From the asymptotic properties of the ML estimator, $\hat{\gamma}_k$ can be considered as a Gaussian random variable such that

$$\hat{\gamma}_k \sim \mathcal{N}(\gamma_k, \sigma_k^2), \quad \sigma_k^2 = [\mathbf{I}_\theta]_{k,k}^{-1} \tag{23}$$

where $\sigma_k^2 \propto \frac{1}{N_r}$ is the estimator variance and $\mathbf{I}_\theta$ is the fisher information matrix [12].

V. Mutual Information

In this section, we consider the mutual information as a performance metric to compare the proposed scheme with the state of the art. We show that the binary asymmetric channel and the multiple-input-single-output (MISO) channel can be used to describe the mutual information of the spatial and modulation symbols, respectively. We provide expressions for the mutual information based on perfect and estimated thresholds. According to the mutual information of the RSM system in equation (22) in [6], the mutual information of the proposed scheme can similarly be expressed as

$$I(\mathbf{s}, x; \hat{\mathbf{s}}, y_c) = I(\mathbf{s}; \hat{\mathbf{s}}) + I(x; y_c|\hat{\mathbf{s}}, \mathbf{s}) \triangleq I_s + I_m \tag{24}$$

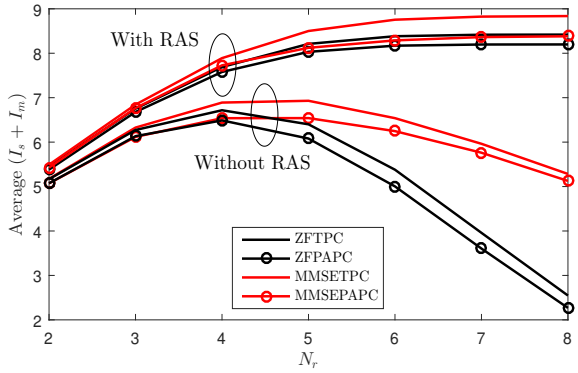

Fig. 2. Mutual information at $L = 16$, $N_t = 32$, SNR $= 5$dB and (average over 1000 channel realizations).

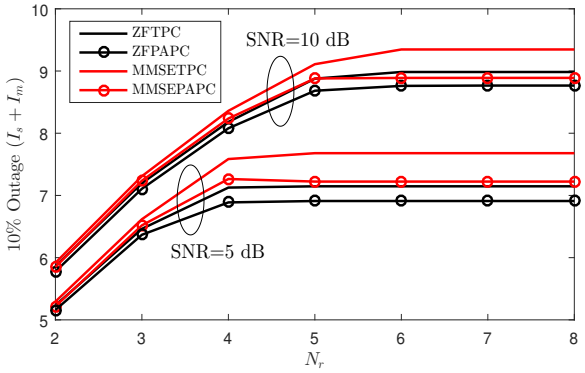

Fig. 3. 10% Outage mutual information with RAS at $L = 16$, $N_t = 32$ and (evaluated over 1000 channel realizations).

where I_s and I_m are the spatial and modulation mutual information, respectively.

A. Spatial symbol mutual information

As we consider independent per antenna spatial detection, the spatial mutual information can be expressed as

$$I_s = \sum_{k=1}^{N_r} I\left(s_k; \hat{s}_k\right) \tag{25}$$

where $I\left(s_k; \hat{s}_k\right)$ can be obtained using the binary asymmetric channel [13] as follows

$$\begin{aligned} I\left(s_k; \hat{s}_k\right) &= \mathcal{H}\left(p_1 P_{1k} + p_0(1 - P_{0k})\right) \\ &\quad - p_1 \mathcal{H}\left(P_{1k}\right) - p_0 \mathcal{H}\left(1 - P_{0k}\right) \end{aligned} \tag{26}$$

where $\mathcal{H}(x)$ is the entropy function [14], $p_1 = \Pr(s_k = 1) = \frac{1}{2}$, $p_0 = \Pr(s_k = 0) = \frac{1}{2}$, and P_{mk} is the probability of the k^{th} antenna to receive $s_k = m$ that can be expressed as

$$P_{mk} = \sum_{i=1}^{2^{N_r - 1}} \Pr\left(a_k \underset{m=0}{\overset{m=1}{\gtrless}} \gamma_k \mid \tilde{\mathbf{s}}_i\right) \Pr\left(\tilde{\mathbf{s}}_i\right) \tag{27}$$

If γ_k is perfectly known at the UT, the probability $\Pr\left(a_k > \gamma_k \mid \tilde{\mathbf{s}}_i\right)$ can be computed using the cumulative density function (CDF) of Rice distribution [11] as follows

$$\Pr\left(a_k > \gamma_k \mid \tilde{\mathbf{s}}_i\right) = Q_1\left(\frac{\sqrt{2}|r_k|}{\sigma}, \frac{\sqrt{2}\gamma_k}{\sigma}\right) \tag{28}$$

The probability $\Pr\left(a_k > \hat{\gamma}_k \mid \tilde{\mathbf{s}}_i\right)$ by considering the estimated threshold in equation (23) can be expressed as

$$\Pr\left(a_k > \hat{\gamma}_k \mid \tilde{\mathbf{s}}_i\right) = \Pr\left(\frac{\hat{\gamma}_k}{a_k} < 1 \mid \tilde{\mathbf{s}}_i\right) = T_{\delta,n,l}\left(\frac{\sigma}{\sigma_k}\right) \tag{29}$$

where $T_{\delta,n,l}(\sigma/\sigma_k)$ is the CDF of doubly-non-central t distribution [15] with $\delta = \frac{\gamma_k}{\sigma_k}$, $n = 2$ and $l = \frac{2|r_k|^2}{\sigma^2}$.

B. Modulation symbol mutual information

Although we consider multiple antennas at the UT, the combined signal at the UT comprises only one modulation symbol that passes through a single RF chain as illustrated in equation (20). Therefore, I_m in equation (24) can be computed using the expression of the mutual information of MISO channel. In [5], the authors showed that the M-phase-shift-keying (M-PSK) constellation can achieve the best performance for the same RSM architecture. Thus, we consider the mutual information expression based M-PSK symbols [16]. From equation (24), I_m can be expressed as

$$I_m = \sum_{i=1}^{2^{N_r}-1} \Pr\left(\mathbf{s}_i\right) \sum_{j=1}^{2^{N_r}} \Pr\left(\hat{\mathbf{s}}_j | \mathbf{s}_i\right) I_{m-\text{MPSK}}\left(x; y_c\right)_{|_{\mathbf{s}_i, \hat{\mathbf{s}}_j}} \tag{30}$$

$$\Pr\left(\hat{\mathbf{s}}_j | \mathbf{s}_i\right) = \prod_{k=1}^{N_r} \Pr\left(a_k \underset{\hat{s}_{jk}=0}{\overset{\hat{s}_{jk}=1}{\gtrless}} \gamma_k \mid \mathbf{s}_i\right), \Pr\left(\mathbf{s}_i\right) = \frac{1}{2^{N_r}} \tag{31}$$

We consider the worst case detection such that

$$I_{m-\text{MPSK}} = \begin{cases} 0 & \text{if } \hat{\mathbf{s}}_j \neq \mathbf{s}_i \\ \frac{1}{2}\log_2 \frac{4\pi}{\mathrm{e}} \frac{\alpha_i^2}{\left(\sum_{k=1}^{N_r} s_{ik}\right)\sigma^2} & \text{if } \hat{\mathbf{s}}_j = \mathbf{s}_i \end{cases} \tag{32}$$

In this case, I_m can be expressed as

$$I_m = \frac{1}{2^{N_r}} \sum_{i=1}^{2^{N_r}-1} \frac{1}{2} \log_2 \frac{4\pi}{\mathrm{e}} \frac{\alpha_i^2}{\left(\sum_{k=1}^{N_r} s_{ik}\right)\sigma^2} \Pr\left(\hat{\mathbf{s}}_i | \mathbf{s}_i\right) \tag{33}$$

VI. Simulation Results

In this section, we compare the performance of the proposed MMSE RSM scheme with the state of the art (ZF RSM) under TPC and PAPC at the BS. A ZF RSM scheme based the energy efficient UT architecture in Fig. 1 has been developed in [5] under TPC and extending this scheme to PAPC can be easily obtained through convex second-order cone programming [17]. In simulations, we consider that $L = 16$, SNR $= P_t/\sigma^2$, $(\phi_i \in [-\pi/6, \pi/6], \theta_i \in [-\pi, \pi])$ are uniformly distributed , $g_i \sim \mathcal{CN}(0, \sigma_g^2)$ and σ_g^2 satisfies $\mathrm{E}\left[\mathrm{Tr}\{\mathbf{H}^H\mathbf{H}\}\right] = N_t N_r$.

Fig. 2 shows the mutual information of the proposed MMSE RSM and the ZF RSM under TPC and PAPC at the BS. The achievable mutual information of the MMSE RSM outperforms that of the ZF RSM specifically at large N_r. This is because the received power in ZF precoding could reach zero when N_r approaches L. Thus, RSM systems with RAS

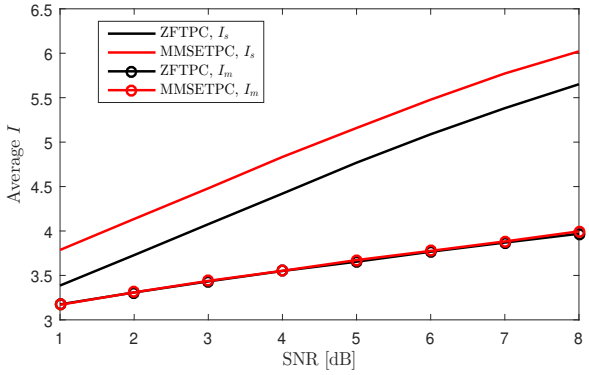

Fig. 4. Mutual information with RAS at $L = 16$, $N_r = 7$, $N_t = 32$ and (average over 1000 channel realizations).

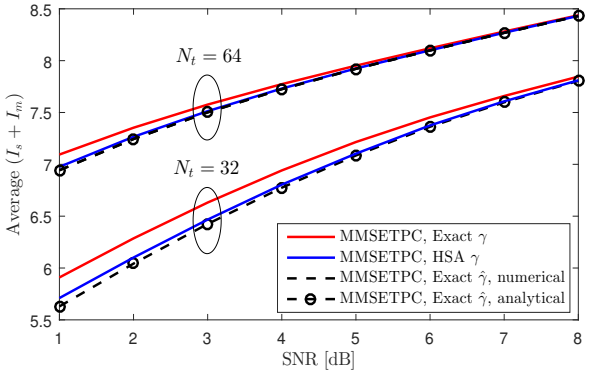

Fig. 5. Mutual information with RAS at $L = 16$, $N_r = 4$ and (average over 1000 channel realizations).

are shown to achieve higher rates that not decrease with N_r. RAS is performed by exhaustive search to maximize its mutual information and updated per the coherence time.

Fig. 3 shows that the 10% outage mutual information of the MMSE RSM outperforms that of the ZF RSM assuming that RAS are performed. Further, at given SNR, there is a number of receive antennas that maximizes the mutual information.

Fig. 4 shows the spatial and modulation mutual information of the (MMSE/ZF) RSM schemes under TPC and RAS assumptions. MMSE precoding achieve higher spatial rates due to its ability to combat the spatial correlation of the channel and hence a larger number of receive antennas can be activated. In MMSE precoding, we can activate more receive antennas than in ZF precoding but each active antenna receives lower power. Thus, the combined signal power in MMSE or ZF is close which leads to similar modulation rates.

Fig. 5 represents the mutual information of the proposed MMSE RSM scheme with TPC and RAS under different thresholds. Not surprisingly, exact threshold is the best and the HSA threshold approaches the rates of the exact threshold with much lower computational complexity and performs well at low SNR. The gap between the perfect and the estimated threshold reduces when N_t or SNR increases.

VII. Conclusion

The proposed MMSE RSM scheme outperforms the ZF RSM because forcing some antennas to receive zero signals could reduce the high level signals received by other antennas which leads to degradation in the mutual information specifically in spatially correlated channels. Simulation results show that there is an optimal number of receive antennas that maximizes the mutual information at given SNR. Thus, we apply RAS method based exhaustive search (computationally complex) to maximize the mutual information. Hence, developing fast and efficient RAS algorithms for MMSE RSM systems is an interesting future research point. It is better to consider the HSA threshold when N_t is large to get the same performance as the exact threshold but with much lower computational complexity. A low number of DL training symbols are needed to estimate the detection thresholds that could be useful for channels with small coherence time.

References

[1] Lie-Liang Yang, "Transmitter preprocessing aided spatial modulation for multiple-input multiple-output systems," *in 73rd IEEE Vehicular Technology Conference (VTC Spring)*, pp. 1–5, May 2011.

[2] A. Stavridis, S. Sinanovic, M. Di Renzo, and H. Haas, "Transmit precoding for receive spatial modulation using imperfect channel knowledge," *in 75th IEEE Vehicular Technology Conference (VTC Spring)*, pp. 1–5, May 2012.

[3] R. Zhang, Lie-Liang Yang, and L. Hanzo, "Generalised pre-coding aided spatial modulation," *IEEE Transactions on Wireless Communications*, vol. 12, no. 11, pp. 5434–5443, Nov. 2013.

[4] N. S. Perovic, P. Liu, M. Di Renzo, and A. Springer, "Receive spatial modulation for LOS mmwave communications based on TX beamforming," *IEEE Communications Letters*, Dec. 2016.

[5] A. Raafat, A. Agustin, and J. Vidal, "Receive spatial modulation for massive MIMO systems," *in IEEE Global Communications Conference (GLOBECOM)*, Dec. 2017.

[6] A. Raafat, A. Agustin, and J. Vidal, "Receive antenna selection and hybrid precoding for receive spatial modulation in massive MIMO systems," *in IEEE International Workshop on Smart Antennas (WSA)*, March 2018.

[7] M. R. Akdeniz et al., "Millimeter wave channel modeling and cellular capacity evaluation," *IEEE Journal on Selected Areas in Communications*, vol. 32, no. 6, pp. 1164–1179, June 2014.

[8] M. Joham, W. Utschick, and J. A. Nossek, "Linear transmit processing in MIMO communications systems," *IEEE Transactions on Signal Processing*, vol. 53, no. 8, pp. 2700–2712, Aug. 2005.

[9] M. Grant and S. Boyd, "Cvx: Matlab software for disciplined convex programming," Sept. 2012.

[10] D. J. Tylavsky and G. R. Sohie, "Generalization of the matrix inversion lemma," *Proceedings of the IEEE*, vol. 74, no. 7, pp. 1050–1052, July 1986.

[11] M. K. Simon, *Probability distributions involving Gaussian random variables: A handbook for engineers and scientists*, Springer, 2007.

[12] H. L. Van Trees, *Optimum Array Processing, Detection, Estimation, and Modulation Theory*, John Wiley & Sons, 2004.

[13] F. Chapeau-Blondeau, "Noise-enhanced capacity via stochastic resonance in an asymmetric binary channel," *Physical Review E*, vol. 55, no. 2, pp. 2016, Feb. 1997.

[14] T. M. Cover and J. A. Thomas, *Elements of Information Theory*, John Wiley & Sons, 2012.

[15] C. Walck, *Handbook on statistical distributions for experimentalists*, University of Stockholm Internal Report, 2007.

[16] P. E. McIllree, *Channel capacity calculations for M-ary N-dimensional signal sets*, Ph.D. thesis, University of South Australia, Feb. 1995.

[17] A. Wiesel, Y. C. Eldar, and S. Shamai, "Zero-forcing precoding and generalized inverses," *IEEE Transactions on Signal Processing*, vol. 56, no. 9, pp. 4409–4418, Sept. 2008.